Near-field GHz rotation and sensing with an optically levitated nanodumbbell

Peng Ju, † Yuanbin Jin, † Kunhong Shen, † Yao Duan, ‡ Zhujing Xu, † Xingyu Gao, † Xingjie Ni, ‡ and Tongcang Li*, † , $^{\P,\S,\parallel}$

†Department of Physics and Astronomy, Purdue University, West Lafayette, Indiana 47907, United States

‡Department of Electrical Engineering, The Pennsylvania State University, University
Park, Pennsylvania 16802, United States

¶Elmore Family School of Electrical and Computer Engineering, Purdue University, West

Lafayette, Indiana 47907, United States

§Birck Nanotechnology Center, Purdue University, West Lafayette, Indiana 47907, United

States

|| Purdue Quantum Science and Engineering Institute, Purdue University, West Lafayette,
Indiana 47907, United States

E-mail: tcli@purdue.edu

Abstract

A levitated non-spherical nanoparticle in vacuum is ideal for studying quantum rotations and is an ultrasensitive torque detector for probing fundamental particle-surface interactions. Here, we optically levitate a silica nanodumbbell in vacuum at 430 nm away from a sapphire surface and drive it to rotate at GHz frequencies. The relative linear speed between the tip of the nanodumbbell and the surface reaches $1.4 \, \mathrm{km \ s^{-1}}$ at a sub-micrometer separation. The rotating nanodumbbell near the surface

demonstrates a torque sensitivity of $(5.0\pm1.1)\times10^{-26}~\mathrm{N}$ m $\mathrm{Hz^{-1/2}}$ at room temperature. Moreover, we probed the near-field laser intensity distribution beyond optical diffraction limit with a nanodumbbell levitated near a nanograting. Our numerical simulations show that the system can measure the Casimir torque and will improve the detection limit of non-Newtonian gravity by several orders of magnitudes.

Keywords: levitated optomechanics, nanorotor, torque sensing, near-field interaction, non-Newtonian gravity, Casimir torque

Main Text

Recently, quantum ground state cooling of the center-of-mass (CoM) motion of an optically levitated nanosphere in vacuum was achieved, 1,2 showing the great potential of levitated nanoparticles for studying macroscopic quantum mechanics.³ Meanwhile, levitated dielectric particles in vacuum are ultrasensitive force detectors, 4 and their CoM motion has been proposed to detect short-range forces, 5-9 dark matter, 10 dark energy, 11 high-frequency gravitational wave, ¹² and quantum gravity. ¹³ Besides the CoM motion, ¹⁴ there is increasing interest in the torsional ¹⁵⁻¹⁷ and rotational motions ¹⁸⁻²¹ of non-spherical particles. ²²⁻²⁴ Levitated non-spherical nanoparticles in free space have been driven to rotate at GHz frequencies, ^{24,25} and cooled by active feedback, ^{26,27} coherent scattering, ²⁸ and spin-optomechanical interaction.²⁹ Theoretical investigations have predicted intriguing quantum revivals³⁰ and quantum persistent tennis racket dynamics³¹ of nanorotors. In addition, a levitated nonspherical nanoparticle in vacuum is an ultrasensitive torque detector 15,32 thanks to its high quality factor and small moment of inertia. It is a rare system that can detect the Casimir torque due to quantum vacuum fluctuations, ^{33,34} search for non-Newtonian interaction, ⁵ and measure the long-sought vacuum friction. 35,36 However, such applications require a nanoparticle to be driven to rotate near a surface at sub-micrometer separations in vacuum, which has not been demonstrated yet.

In this article, we optically levitate a nanodumbbell 24 at a sub-micrometer separation from a surface for the first time, and drive it to rotate at 1.6 GHz near the surface in a high vacuum. Despite a small particle-surface separation of 430 nm, we achieve stable GHz rotation of a nanodumbbell near a surface without external feedback cooling. The standing wave $^{37-39}$ formed near the surface due to surface reflection provides stronger spatial confinement than the optical tweezers in free space, which helps to stabilize the trapping. For a nanodumbbell consists of two silica nanospheres with diameters of 144 nm, this mechanical rotation corresponds to a linear speed of 1.4 km s⁻¹ at the tip of the nanodumbbell relative to the surface. Such a record-high relative speed at a sub-micrometer separation is ideal for detecting the long-sought vacuum friction. 35,36

We also measure the torque sensitivity and three-dimensional force sensitivity of a nanodumbbell levitated near a sapphire surface. The nanodumbbell near the surface demonstrates a torque sensitivity of $(5.0\pm1.1)\times10^{-26}$ N m Hz^{-1/2} at 6.1×10^{-5} Torr at room temperature. Thus, a levitated nanoparticle near a surface is ideal for investigating fundamental particle-surface interactions. As an example of potential applications, we levitate a nanodumbbell in the first trapping well near a gold nanograting with a nanostrip width of 300 nm and detect the near-field interference of the trapping laser beyond the optical diffraction limit. In addition, our system will be sensitive enough to measure the Casimir torque with torsional free-fall experiment. 33,40 Our numerically simulations predict a nanodumbbell levitated near a nanostrip will set a new limit on non-Newtonian gravity. Our work is an important development in levitated optomechanics. It shows a levitated nanodumbbell near a surface in vacuum will be able to probe surface interactions with ultrahigh torque and force sensitivities that are not achievable with conventional atomic force microscopes.

In the experiment, we first levitate a silica nanodumbbell with a tightly focused 1550 nm laser in free space (See Supporting Information S1 for details). The laser power at the trapping region is about 200 mW. A levitated nanodumbbell shows a large torsional peak from the power spectrum density (PSD) and its geometry can be confirmed by measuring

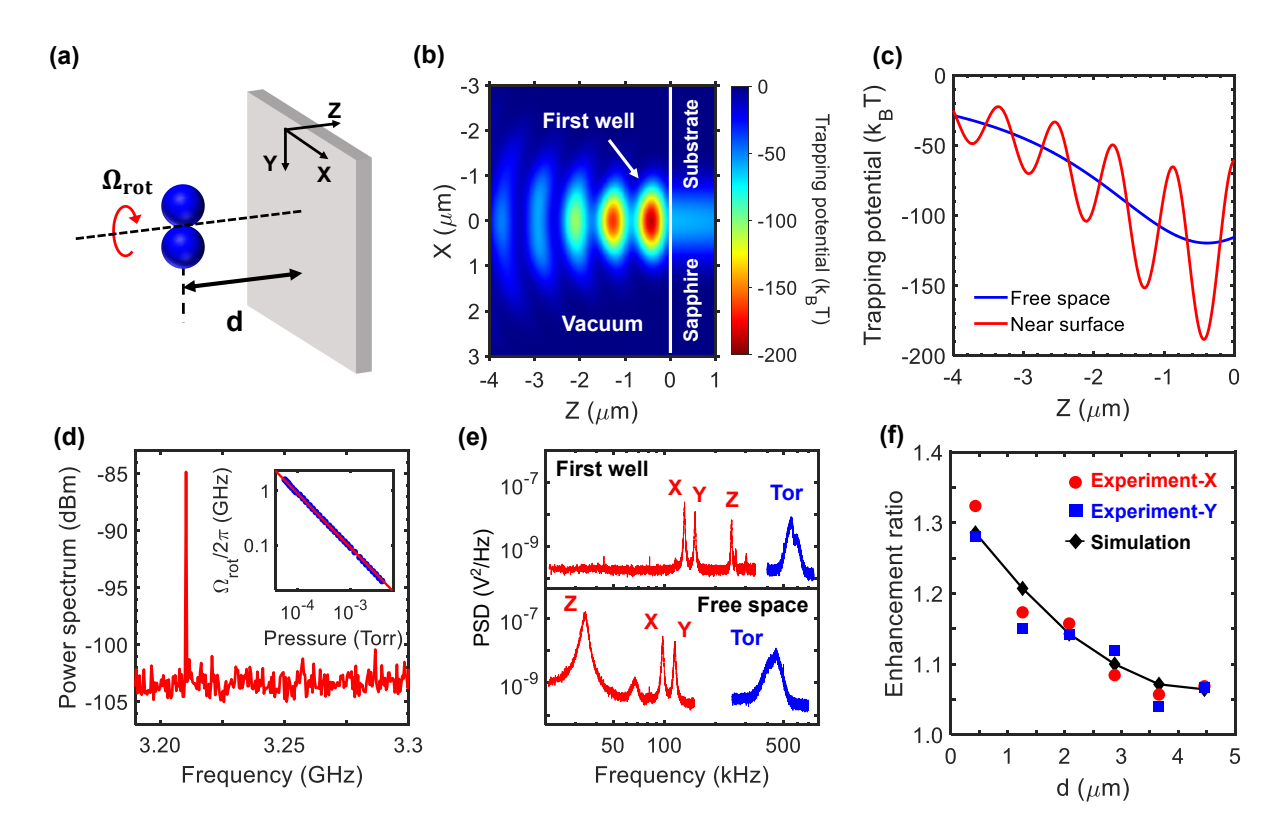


Figure 1. Optical levitation and GHz rotation of a nanodumbbell near a sapphire surface. (a) Schematic of a nanodumbbell rotating at a separation of d from the sapphire surface. (b) Simulated trapping potential for a nanodumbbell levitated near the sapphire surface in the unit of k_BT (T = 300 K). Discrete trapping wells are formed due to the standing wave effect near the surface. The trapping position of the first well is about 430 nm from the surface. (c) Analytically calculated trapping potential of a nanodumbbell along the propagation direction of the trapping laser. The red and blue curves are trapping potentials near the sapphire surface and in free space, respectively. (d) Measured power spectrum of the rotational signal of a nanodumbbell trapped in the first well near the sapphire surface. The peak near 3.2 GHz corresponds to a mechanical rotation frequency of 1.6 GHz at the pressure of 5.9×10^{-5} Torr. The inset figure shows the measured rotation frequency as a function of pressure (blue dot) and a fitting curve (solid red line) proportional to 1/P, where P is the pressure. (e) PSDs of a nanodumbbell trapped in the first well near the sapphire surface (top) and in free space (bottom) at 1.5 Torr. The trapping laser is linearly polarized. The oscillation frequencies of the CoM (Red) and torsional (Blue) motions in the first well are significantly larger than those in free space. (f) Enhancement ratios of the oscillation frequencies of a nanodumbbell levitated at discrete trapping wells near a sapphire surface over that in free space. Red dots and blue squares are measured enhancement ratios for X and Y motions a function of the distance from the sapphire surface, respectively. The simulation results (black diamonds) are calculated based on the simulated trapping potential shown in (b).

damping rate ratio of the CoM motion. 24 Then, a high voltage source creates air discharge to neutralize the nanodumbbell (Figure S2). After neutralization, a sapphire surface is inserted perpendicularly to the axis of the trapping laser, and the nanodumbbell will be trapped near the sapphire surface (Figure 1a). The partly reflected laser from the surface interferes with the original trapping laser and forms a partial standing wave. This creates discrete trapping wells near the sapphire surface, as shown in Figure 1(b-c). The nanodumbbell near the sapphire surface is trapped in one of the trapping wells. By controlling the surface position along the z direction before inserting the sapphire substrate, we can determistically load the nanodumbbell into different trapping wells near the surface. The equilibrium positions of the trapping wells are located at the anti-nodes of the standing waves. The separation between the equilibrium position of the first trapping well and the surface is about 430 nm. It is not exactly $\lambda/4$ because the laser is a focused beam instead of a parallel beam.

After the nanodumbbell is trapped in the first well near the sapphire surface, we apply optical torque on the nanodumbbell with the angular momentum of the circularly polarized trapping laser and drives it to rotate in vacuum. The rotation frequency is determined by the balance of optical torque and the frictional torque from the residual air given by $-I\gamma\Omega_{rot}$. Here I is the moment of inertia of the nanodumbbell, γ is the rotational damping rate and Ω_{rot} is the angular velocity. While the optical torque is independent of the pressure, the rotational damping rate is proportional to the air pressure P. Therefore, the rotation frequency is inversely proportional to the P, as shown in the inset of Figure 1d. At 5.9×10^{-5} Torr, the mechanical rotation frequency of the nanodumbbell reaches 1.6 GHz (Figure 1d). This corresponds to a linear velocity of 1.4 km s⁻¹ between the tip of the nanodumbbell and the sapphire surface, separated by 430 nm. While a nanosphere has been levitated near a surface before, ^{7.8,41} to our best knowledge, this is the first report on optical levitation and GHz rotation of a non-spherical nanoparticle near a surface. Such a levitated GHz nanorotor near a surface can be used to explore fundamental physics like measuring quantum friction. ^{35,36}

As a result of the standing wave potential, both the CoM motion and torsional motion of a nanodumbbell levitated near the surface is significantly different from free space (Figure 1e). In particular, the oscillation frequency of the CoM motion along the z direction (f_z) is enhanced by about 7 times from 35 kHz to 250 kHz. The enhanced trapping frequencies indicate stronger spatial confinement for a nanodumbbell levitated near a sapphire surface than in free space. The root-mean-square (RMS) values of the z position for a nanodumbbell levitated in the first well and free space are 15 nm and 109 nm, respectively (Figure S3). The spatial squeezing along the z direction is crucial for stably trapping a nanodumbbell close to a surface, especially at a high vacuum. Besides the stronger confinement of z motion, the oscillation frequencies of x, y and torsional motions are also enhanced by the increased laser intensity gradient due to surface reflection. In the experiment, we measure frequency enhancement ratio of x and y motions as a function of the particle-surface distance: $f_{x,y}(d)/f_{free\ space}$ (Figure 1f). The experimental results agree well with the calculated enhancement ratio using the simulated trapping potential, showing we have indeed trapped the nanodumbbell near the sapphire surface.

An important motivation for levitating a nanodumbbell near the surface is to study fundamental particle-surface interactions by ultrasensitive torque and force detection. For this purpose, we measure the torque sensitivity and 3D force sensitivity of a levitated nanodumbbell near the sapphire surface. For a nanodumbbell levitated in free space, the torque and force sensitivities are limited by the thermal noise from the residual air in the vacuum chamber and photon shot noise from the trapping laser. When the nanodumbbell is brought close to a surface, its torque and force sensitivities might potentially be affected by the surface. ^{42,43}

Here we measure the torque sensitivity (Figure 2c) and rotational damping time (Figure 2b) as a function of pressure for a rotating nanodumbbell levitated in the first well and in free space. The rotational damping time of the nanodumbbell is measured with the ring-up experiment (Figure S4 and Figure S5). The damping time remains nearly the same when the

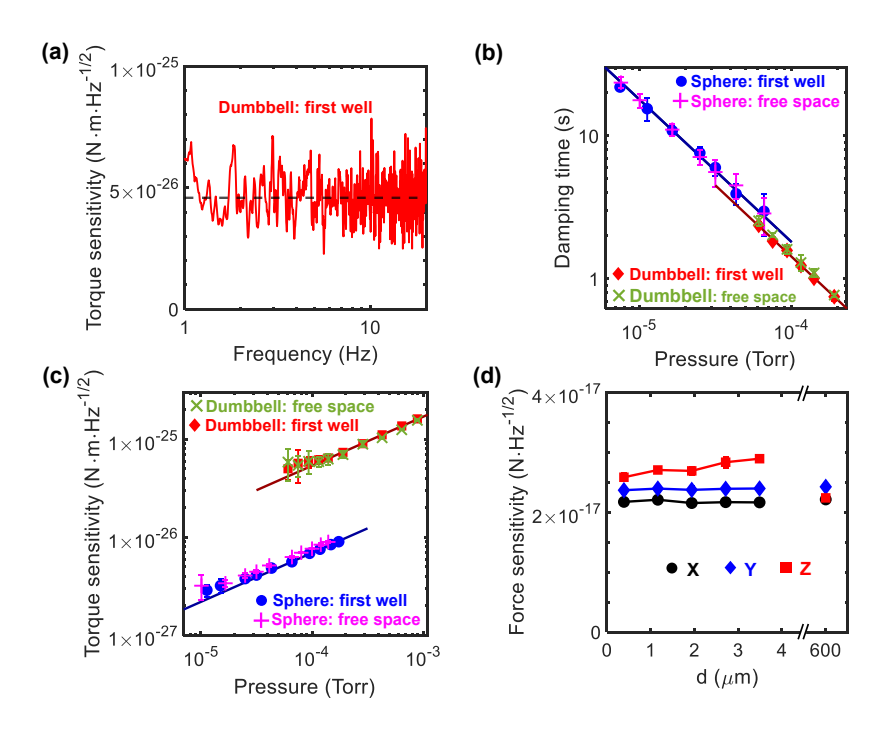


Figure 2. Torque and force sensing with a nanodumbbell levitated near a sapphire surface. (a) Torque sensitivity of a nanodumbbell levitated in the first well near a sapphire surface as a function of frequency at 6.1×10^{-5} Torr. The dash line shows an average torque sensitivity of 4.6×10^{-26} N m Hz^{-1/2} for this single measurement. (b) Damping time (τ) of a nanodumbbell in the first well (red diamond) and in free space (green cross), a nanosphere levitated in the first well (blue circle), and free space (magenta plus sign). The dark blue and dark red lines are fitting curves based on $\tau \propto 1/P$ for a nanodumbbell and a nanosphere levitated in the first well (red diamond) and in free space (green cross), a nanosphere levitated in the first well (blue circle), and in free space (magenta plus sign). The dark blue and dark red lines are fitting curves based on $S_T^{1/2} \propto \sqrt{P}$ for a nanodumbbell and a nanosphere levitated in the first well, respectively. (d) Three-dimensional force sensitivity of a nanodumbbell as a function of distance to the surface.

nanodumbbell is brought from free space to the first well near a surface, indicating no extra damping from the sapphire surface. If a nanoparticle is trapped in a liquid, the damping rate will increase when it is close to a surface. ⁴² In contrast, the damping rate due to residual air molecules at low pressures is insensitive to the separation when the mean free path of molecules is much larger than the size of the nanoparticle and the separation. ⁴³ The torque sensitivity ³² of a nanodumbbell as a function of frequency is $S_T^{1/2}(\omega) = I\sqrt{\gamma^2 + \omega^2} S_{noise}^{1/2}(\omega)$. $S_{noise}^{1/2}(\omega)$ is the single-sided PSD of Ω_{rot} due to thermal (Brownian) rotation. The details of

determining torque sensitivity are presented in Section 3 of the Supplementary Information. For the same nanodumbbell, the difference in the torque sensitivity between levitating near the surface and in free space is within the measurement uncertainty. The torque sensitivities are limited by the air damping and are proportional to \sqrt{P} at high pressure. At 6.1×10^{-5} Torr, the torque sensitivity of a nanodumbbell levitated near the surface reaches $(5.0\pm1.1)\times10^{-26}$ N m Hz^{-1/2}. In addition, we perform the same measurement of damping time and torque sensitivity on a nanosphere, which shows a similar trend as a function of pressure. Compared to a nanodumbbell composed of two nanospheres, a single nanosphere has a smaller moment of inertia, resulting in a better torque sensitivity than a nanodumbbell at the same pressure. However, an isotropic nanosphere will not experience a Casimir torque that requires asymmetry. Therefore, the nanodumbbell is a better candidate for measuring the Casimir torque than a nanosphere.

The 3D force sensitivity of a nanodumbbell levitated at 1.5 Torr is measured as a function of the separation from the surface (Figure 2d). From the experiment results, the force sensitivity of the nanodumbbell is insensitive to the distance between the nanodumbbell and the surface, in consistent with our results of the torque sensitivity. The average force sensitivity of a nanodumbbell along all three directions is about 2.5×10^{-17} N Hz^{-1/2} at 1.5 Torr. The sensitivity will increase further when the pressure decreases. Thus, a levitated nanodumbbell near a surface can also be used for 3D near-field force microscopy.⁶

In addition to trapping near a flat sapphire surface, we also levitate a nanodumbbell near a gold nanograting and probe subwavelength light field near the nanograting. The nanograting is composed of periodical gold nanostrips on a sapphire substrate (Figure 3a). The period of the nanograting is 600 nm, and the width of each gold nanostrip is 300 nm. The nanostrips of the nanograting cannot be observed from the optical image shown in Figure 3b as their feature size is smaller than the diffraction limit of our optical imaging system. When the 1550 nm laser is focused on the nanograting, the reflected laser from adjacent gold nanostrips interferes and changes the laser intensity distribution along the x

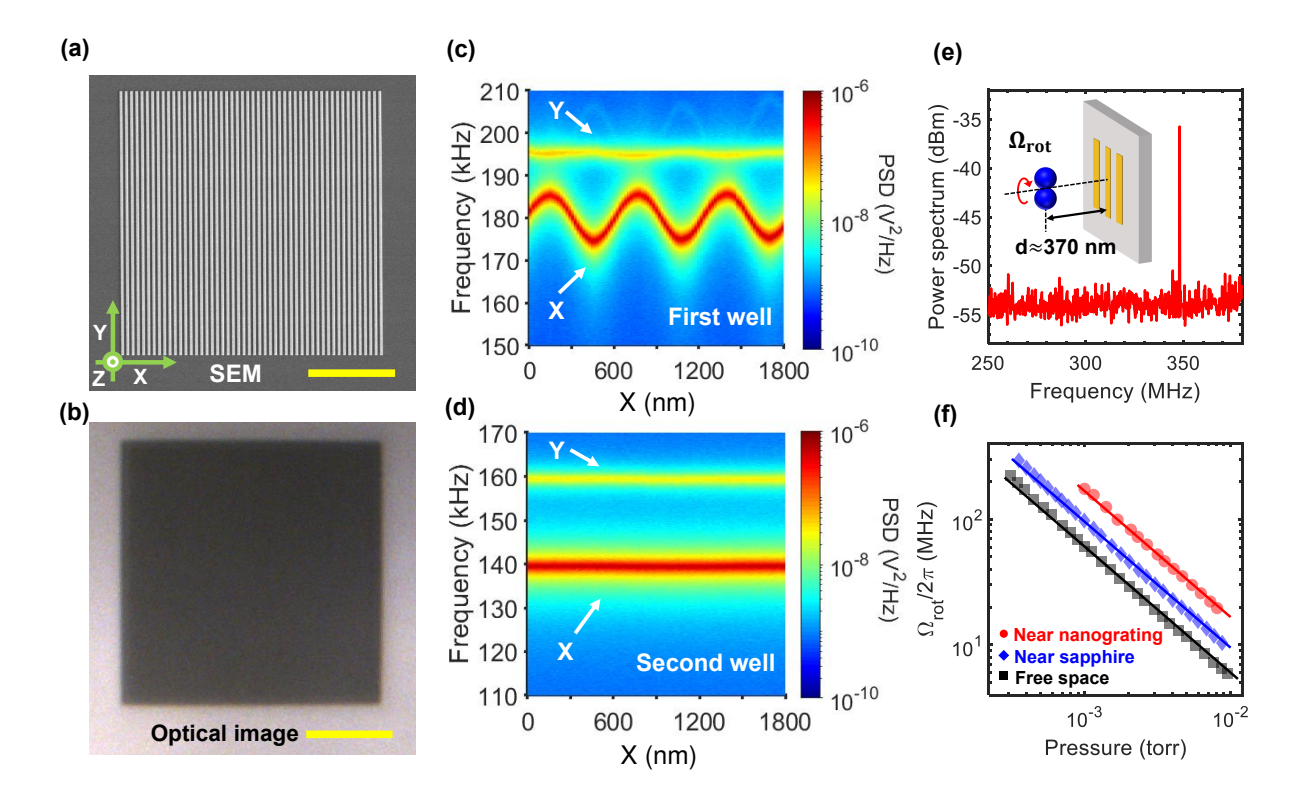


Figure 3. Sensing and rotation of a nanodumbbell near a nanograting. (a) SEM and (b) optical image of a gold nanograting with a grating period of 600 nm. The width of each gold nanostrip in the nanograting is 300 nm. The yellow scale bar corresponds to a length of 10 μ m. (c) and (d) are the measured PSDs of a nanodumbbell scanning along the x direction when it is trapped in the first and second trapping wells near the nanograting surface, respectively. The frequency change in the first well measures the near-field intensity distribution of the nanograting. (e) Power spectrum of the rotation of a nanodumbbell near the nanograting. Inset is the schematic diagram. The peak at 350 MHz corresponds to a rotation frequency of 175 MHz at 1.0×10^{-3} Torr. (f) Rotation frequency of the nanodumbbell as a function of air pressure when it is levitated in the first well near the nanograting (red dot), in the first well near a flat sapphire surface (blue diamond) and in free space (black square). The solid lines are fitting curves proportional to 1/P.

direction (Figure S6). As the nanograting period is much smaller than the trapping laser wavelength, such interference only exists in the near-field region and cannot be detected with far-field detectors. The CoM motion of a levitated nanodumbbell is sensitive to the laser intensity distribution near the trapping region. To study the near-field diffraction of the nanograting, we scan the nanograting with a nanodumbbell trapped in the first well near the nanograting. The oscillation frequency of x motion changes periodically when the

nanodumbbell scans in the first well (Figure 3c), while the frequency remains nearly constant when the nanodumbbell scans in the second well (Figure 3d). This shows that the near-field interference disappears at a separation of 1.2 μ m from the nanograting surface.

After trapping a nanodumbbell in the first well near the nanograting, we drive it to rotate in vacuum with the circularly polarized trapping laser. At 1.0×10^{-3} Torr, the rotational frequency of the nanodumbbell levitated near nanograting reaches 175 MHz. Figure 3f shows the rotation frequency as a function of pressure for the same nanodumbbell trapped in the first well near a flat sapphire surface, in the first well near nanograting, and in free space. For all three cases, the rotation frequency follows the 1/P dependence, as air damping is the dominant damping source. The difference between the rotation frequencies for different configurations at the same pressure is caused by different amounts of reflection from the surface, which changes the optical torque. The nanodumbbell levitated near the nanograting has the highest rotation frequency among these three situations at a given pressure due to the high reflectivity of the gold nanograting. In addition, we have levitated a nanodumbbell near a gold micro-disk (Figure S7), which shows an even larger enhancement in trapping frequencies.

According to quantum electrodynamics, the vacuum is not empty but full of virtual photons (quantum vacuum fluctuations). The quantum vacuum fluctuations can lead to an attractive force between neutral plates in vacuum, known as the Casimir force. 46 If the plates are optically anisotropic, vacuum fluctuations can also induce a torque between them. 47 While the Casimir force has been measured extensively, 48,49 the Casimir torque has only been measured with liquid crystals at small separations. 34 A nanodumbbell levitated near a nanograting will provide an opportunity to study the Casimir torque at different separations systematically, 33,50 especially at separations when the retardation effect is important. A nanograting not only causes near-field interference of real photons but also breaks the rotational symmetry of virtual photons near it, 50 producing a Casimir torque along the rotation axis. Due to the complex geometry, the Casimir torque between a levitated nanodumbbell

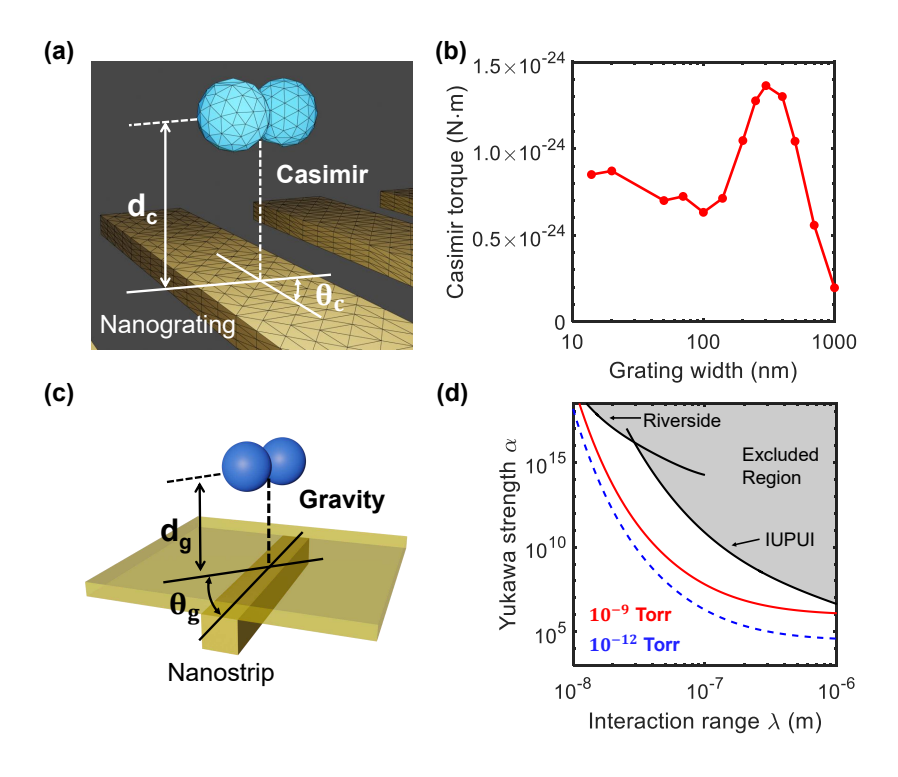


Figure 4. Protocols to measure Casimir torque and search for non-Newtonian gravity with a nanodumbbell levitated near nanostructures. (a) Schematic diagram of measuring Casimir torque with a nanodumbbell levitated near the nanograting. The finite element mesh is applied to simulate the Casimir torque. d_c is the distance between the center of nanodumbbell and the top-surface of the nanograting. θ_c is the relative angle between a gold nanostrip in the nanograting and the long axis of the nanodumbbell. (b) Simulated Casimir torque as a function of grating width for a fixed $d_c = 370$ nm and $\theta_c = 135$ deg. (c) Schematic diagram of exploring non-Newtonian gravity with a nanodumbbell levitated near a nanostrip. The gold nanostrip has a dimension of $0.4 \times 0.4 \times 10 \ \mu \text{m}^3$. A gold film with the thickness of 150 nm on top of the nanotrip is used to screen the Casimir effect between the nanostrip and nanodumbbell. d_q is the separation between the center of the nanodumbbell and the top surface of the gold film. θ_q is the relative angle between the long axis of the nanodumbbell and the long axis of the nanostrip. When θ_g is non-zero, there is a gravity induced torque on the nanodumbbell to rotate the nanodumbbell towards $\theta_q = 0$. (d), Detection limits in λ and α phase space for a nanodumbbell levitated near a nanostrip at different pressures. The gray region is excluded by the former experiment from UC Riverside⁴⁴ and IUPUI. 45 $d_q =$ 250 nm is used for the calculation. The red solid curve and blue dash curve correspond to the theoretical detection limit of the nanodumbbell at 10^{-9} Torr and 10^{-12} Torr.

and a nanostructure has not been calculated before.

Here we numerically calculate the Casimir effect between a nanodumbbell and a gold nanograting (Figure 4a) with SCUFF-CAS3D codes (see Supporting Information S5 for de-

tails). The nanograting can affect both spin and spatial distribution of vacuum fluctuations, inducing novel effects that do not exist for natural birefringent crystals. 36,48 Our calculated Casimir torque on the nanodumbbell shows a strong dependence on the width of the nanograting, as shown in Figure 4b. At the separation of 370 nm, the maximum Casimir torque happens when the grating width is about 300 nm. The calculated Casimir torque is 1.4×10^{-24} N m for $\theta = 135$ deg and d = 370 nm, which is one order larger than our measured torque sensitivity of a nanodumbbell (Figure 2a). We numerically simulated the torsional free-fall experiment (Figure S9) 33,51 for a nanodumbbell in the presence of Casimir torque. The simulations show that this system is sensitive enough to detect the Casimir torque on the nanodumbbell.

In addition to detecting Casimir torque, a nanodumbbell levitated near a nanostrip can significantly improve the existing Yukawa strength limit for the search of non-Newtonian interaction at sub-micrometer separation 44,45 (Figure 4c). Similar to the principle of Cavendish torsion balance, torsional measurement of gravity using a nanodumbbell is more robust to gravitational perturbations from the environment than force measurement with the COM motion (Table S1). The non-Newtonian gravitational potential between two point mass M_1 and M_2 separated by a distance d is given by $U(d) = -G\frac{M_1M_2}{d}(1+\alpha e^{-d/\lambda})$, where α and λ are the Yukawa strength and interaction range of non-Newtonian interaction, correspondingly. In our protocol of measuring non-Newtonian gravity, a sub-micrometer scale test mass (nanodumbbell with a sphere radius of 200 nm) is stably levitated at a sub-micrometer separation from the source mass (nanostrip), thanks for the near-field standing wave trapping potential. For each interaction range λ , the detection limit of Yukawa strength α is calculated based on the torque sensitivity of the nanodumbbell using finite element method (See section 6 of the Supporting Information for details). From the numerical calculation, our protocol can improve the current detecting limit of the non-Newtonian interaction by several orders of magnitude from 10 nm to 1 μm .

In summary, we have demonstrated near-field GHz mechanical rotation with a nan-

odumbbell levitated by optical tweezers at about 430 nm from a sapphire surface. The standing wave formed by the reflection of the optical tweezers from the surface provides a stable trapping potential near the surface, where a nanodumbbell is stably trapped and driven to rotate in a high vacuum without feedback cooling. The nanodumbbell maintains its superior torque and force sensitivities at sub-micrometer separation from a surface. We achieve a torque sensitivity of 5.0×10^{-26} N m Hz^{-1/2} and a 3D force sensitivity of 2.5×10^{-17} N Hz^{-1/2} with a nanodumbbell levitated near the surface. We also trap a nanodumbbell near a gold nanograting and use it to detect the near-field laser intensity distribution beyond the diffraction limit. Our simulation shows this system is sensitive enough to detect the Casimir torque and search for non-Newtonian gravity with a nanodumbbell levitated near nanostructures.

Acknowledgement

We thank Alejandro J. Grine, Francis Robicheaux and Jonghoon Ahn for helpful discussions. We acknowledge the support from the Office of Naval Research under Grant No. N00014-18-1-2371 and National Science Foundation under Grant PHY-2110591. This project is also partially supported by the Laboratory Directed Research and Development program at Sandia National Laboratories, a multimission laboratory managed and operated by National Technology and Engineering Solutions of Sandia LLC, a wholly owned subsidiary of Honeywell International Inc., for the U.S. Department of Energy's National Nuclear Security Administration under Contract No. DE-NA0003525. This paper describes objective technical results and analysis. Any subjective views or opinions that might be expressed in the paper do not necessarily represent the views of the U.S. Department of Energy or the United States Government.

Supporting Information Available

Details of experimental setup and methods, charge control of levitated nanoparticle, spatial distribution of the CoM position, torque sensitivity measurement, trapping near nanograting and micro-disk, Casimir force near a nanograting, numerical simulation of torsinoal free fall experiment. (PDF)

References

- (1) Delić, U.; Reisenbauer, M.; Dare, K.; Grass, D.; Vuletić, V.; Kiesel, N.; Aspelmeyer, M. Cooling of a levitated nanoparticle to the motional quantum ground state. <u>Science</u> **2020**, 367, 892–895.
- (2) Piotrowski, J.; Windey, D.; Vijayan, J.; Gonzalez-Ballestero, C.; de los Ríos Sommer, A.; Meyer, N.; Quidant, R.; Romero-Isart, O.; Reimann, R.; Novotny, L. Simultaneous ground-state cooling of two mechanical modes of a levitated nanoparticle. Nature Physics 2023, https://doi.org/10.1038/s41567-023-01956-1.
- (3) Gonzalez-Ballestero, C.; Aspelmeyer, M.; Novotny, L.; Quidant, R.; Romero-Isart, O. Levitodynamics: Levitation and control of microscopic objects in vacuum. <u>Science</u> **2021**, 374, eabg3027.
- (4) Liang, T.; Zhu, S.; He, P.; Chen, Z.; Wang, Y.; Li, C.; Fu, Z.; Gao, X.; Chen, X.; Li, N.; Zhu, Q.; Hu, H. Yoctonewton force detection based on optically levitated oscillator. Fundamental Research **2023**, 3, 57–62.
- (5) Geraci, A. A.; Papp, S. B.; Kitching, J. Short-Range Force Detection Using Optically Cooled Levitated Microspheres. Phys. Rev. Lett. 2010, 105, 101101.
- (6) Blakemore, C. P.; Rider, A. D.; Roy, S.; Wang, Q.; Kawasaki, A.; Gratta, G. Three-

- dimensional force-field microscopy with optically levitated microspheres. Phys. Rev. A **2019**, 99, 023816.
- (7) Diehl, R.; Hebestreit, E.; Reimann, R.; Tebbenjohanns, F.; Frimmer, M.; Novotny, L. Optical levitation and feedback cooling of a nanoparticle at subwavelength distances from a membrane. Phys. Rev. A 2018, 98, 013851.
- (8) Montoya, C.; Alejandro, E.; Eom, W.; Grass, D.; Clarisse, N.; Witherspoon, A.; Geraci, A. A. Scanning force sensing at micrometer distances from a conductive surface with nanospheres in an optical lattice. Appl. Opt. 2022, 61, 3486–3493.
- (9) Agrenius, T.; Gonzalez-Ballestero, C.; Maurer, P.; Romero-Isart, O. Interaction between an Optically Levitated Nanoparticle and Its Thermal Image: Internal Thermometry via Displacement Sensing. Phys. Rev. Lett. 2023, 130, 093601.
- (10) Afek, G.; Carney, D.; Moore, D. C. Coherent Scattering of Low Mass Dark Matter from Optically Trapped Sensors. Phys. Rev. Lett. **2022**, 128, 101301.
- (11) Yin, P.; Li, R.; Yin, C.; Xu, X.; Bian, X.; Xie, H.; Duan, C.-K.; Huang, P.; He, J.-h.; Du, J. Experiments with levitated force sensor challenge theories of dark energy. Nature Physics 2022, 18, 1181–1185.
- (12) Aggarwal, N.; Winstone, G. P.; Teo, M.; Baryakhtar, M.; Larson, S. L.; Kalogera, V.; Geraci, A. A. Searching for New Physics with a Levitated-Sensor-Based Gravitational-Wave Detector. Phys. Rev. Lett. 2022, 128, 111101.
- (13) Bose, S.; Mazumdar, A.; Morley, G. W.; Ulbricht, H.; Toroš, M.; Paternostro, M.; Geraci, A. A.; Barker, P. F.; Kim, M. S.; Milburn, G. Spin Entanglement Witness for Quantum Gravity. Phys. Rev. Lett. 2017, 119, 240401.
- (14) Rieser, J.; Ciampini, M. A.; Rudolph, H.; Kiesel, N.; Hornberger, K.; Stickler, B. A.;

- Aspelmeyer, M.; Delić, U. Tunable light-induced dipole-dipole interaction between optically levitated nanoparticles. Science **2022**, 377, 987–990.
- (15) Hoang, T. M.; Ma, Y.; Ahn, J.; Bang, J.; Robicheaux, F.; Yin, Z.-Q.; Li, T. Torsional Optomechanics of a Levitated Nonspherical Nanoparticle. Phys. Rev. Lett. **2016**, <u>117</u>, 123604.
- (16) Ma, Y.; Hoang, T. M.; Gong, M.; Li, T.; Yin, Z.-q. Proposal for quantum many-body simulation and torsional matter-wave interferometry with a levitated nanodiamond. Phys. Rev. A 2017, 96, 023827.
- (17) Xiao, K.-W.; Xiong, A.; Zhao, N.; Yin, Z.-q. Quantum ground state cooling of translational and librational modes of an optically trapped nanoparticle coupling cavity. Quantum Engineering 2021, 3, e62.
- (18) Stickler, B. A.; Hornberger, K.; Kim, M. S. Quantum rotations of nanoparticles. <u>Nature</u> Reviews Physics **2021**, 3, 589–597.
- (19) Matos, G. C.; Souza, R. d. M. e.; Neto, P. A. M.; Impens, F. m. c. Quantum Vacuum Sagnac Effect. Phys. Rev. Lett. **2021**, 127, 270401.
- (20) Li, J.; Kollipara, P. S.; Liu, Y.; Yao, K.; Liu, Y.; Zheng, Y. Opto-Thermocapillary Nanomotors on Solid Substrates. ACS Nano **2022**, 16, 8820–8826.
- (21) Jin, Y.; Yan, J.; Rahman, S. J.; Li, J.; Yu, X.; Zhang, J. 6 GHz hyperfast rotation of an optically levitated nanoparticle in vacuum. Photon. Res. **2021**, 9, 1344–1350.
- (22) Kuhn, S.; Kosloff, A.; Stickler, B. A.; Patolsky, F.; Hornberger, K.; Arndt, M.; Millen, J. Full rotational control of levitated silicon nanorods. Optica **2017**, 4, 356–360.
- (23) Yan, J.; Yu, X.; Han, Z. V.; Li, T.; Zhang, J. On-demand assembly of optically levitated nanoparticle arrays in vacuum. Photon. Res. **2023**, 11, 600–608.

- (24) Ahn, J.; Xu, Z.; Bang, J.; Deng, Y.-H.; Hoang, T. M.; Han, Q.; Ma, R.-M.; Li, T. Optically Levitated Nanodumbbell Torsion Balance and GHz Nanomechanical Rotor. Phys. Rev. Lett. **2018**, 121, 033603.
- (25) Reimann, R.; Doderer, M.; Hebestreit, E.; Diehl, R.; Frimmer, M.; Windey, D.; Tebben-johanns, F.; Novotny, L. GHz Rotation of an Optically Trapped Nanoparticle in Vacuum. Phys. Rev. Lett. 2018, 121, 033602.
- (26) Bang, J.; Seberson, T.; Ju, P.; Ahn, J.; Xu, Z.; Gao, X.; Robicheaux, F.; Li, T. Five-dimensional cooling and nonlinear dynamics of an optically levitated nanodumbbell. Phys. Rev. Res. 2020, 2, 043054.
- (27) van der Laan, F.; Tebbenjohanns, F.; Reimann, R.; Vijayan, J.; Novotny, L.; Frimmer, M. Sub-Kelvin Feedback Cooling and Heating Dynamics of an Optically Levitated Librator. Phys. Rev. Lett. 2021, 127, 123605.
- (28) Schäfer, J.; Rudolph, H.; Hornberger, K.; Stickler, B. A. Cooling Nanorotors by Elliptic Coherent Scattering. Phys. Rev. Lett. **2021**, 126, 163603.
- (29) Delord, T.; Huillery, P.; Nicolas, L.; Hétet, G. Spin-cooling of the motion of a trapped diamond. Nature **2020**, 580, 56–59.
- (30) Stickler, B. A.; Papendell, B.; Kuhn, S.; Schrinski, B.; Millen, J.; Arndt, M.; Hornberger, K. Probing macroscopic quantum superpositions with nanorotors. <u>New Journal</u> of Physics **2018**, 20, 122001.
- (31) Ma, Y.; Khosla, K. E.; Stickler, B. A.; Kim, M. S. Quantum Persistent Tennis Racket Dynamics of Nanorotors. Phys. Rev. Lett. **2020**, 125, 053604.
- (32) Ahn, J.; Xu, Z.; Bang, J.; Ju, P.; Gao, X.; Li, T. Ultrasensitive torque detection with an optically levitated nanorotor. Nature Nanotechnology **2020**, 15, 89–93.

- (33) Xu, Z.; Li, T. Detecting Casimir torque with an optically levitated nanorod. Phys. Rev. A 2017, 96, 033843.
- (34) Somers, D. A. T.; Garrett, J. L.; Palm, K. J.; Munday, J. N. Measurement of the Casimir torque. Nature **2018**, 564, 386–389.
- (35) Pendry, J. B. Shearing the vacuum-quantum friction. <u>Journal of Physics: Condensed</u>
 Matter **1997**, 9, 10301.
- (36) Xu, Z.; Jacob, Z.; Li, T. Enhancement of rotational vacuum friction by surface photon tunneling. Nanophotonics **2021**, 10, 537–543.
- (37) Čižmár, T.; Garcés-Chávez, V.; Dholakia, K.; Zemánek, P. Optical conveyor belt for delivery of submicron objects. Applied Physics Letters **2005**, 86, 174101.
- (38) Brzobohatý, O.; Karásek, V.; Siler, M.; Chvátal, L.; Cižmár, T.; Zemánek, P. Experimental demonstration of optical transport, sorting and self-arrangement using a 'tractor beam'. Nature Photonics **2013**, 7, 123–127.
- (39) Grass, D.; Fesel, J.; Hofer, S. G.; Kiesel, N.; Aspelmeyer, M. Optical trapping and control of nanoparticles inside evacuated hollow core photonic crystal fibers. <u>Applied</u> Physics Letters **2016**, 108, 221103.
- (40) Antezza, M.; Chan, H. B.; Guizal, B.; Marachevsky, V. N.; Messina, R.; Wang, M. Giant Casimir Torque between Rotated Gratings and the $\theta=0$ Anomaly. Phys. Rev. Lett. **2020**, 124, 013903.
- (41) Magrini, L.; Norte, R. A.; Riedinger, R.; Marinković, I.; Grass, D.; Delić, U.; Gröblacher, S.; Hong, S.; Aspelmeyer, M. Near-field coupling of a levitated nanoparticle to a photonic crystal cavity. Optica 2018, 5, 1597–1602.
- (42) Rogers, S. A.; Lisicki, M.; Cichocki, B.; Dhont, J. K. G.; Lang, P. R. Rotational Diffusion of Spherical Colloids Close to a Wall. Phys. Rev. Lett. **2012**, 109, 098305.

- (43) Ramanathan, S.; Koch, D. L.; Bhiladvala, R. B. Noncontinuum drag force on a nanowire vibrating normal to a wall: Simulations and theory. Physics of Fluids **2010**, 22, 103101.
- (44) Harris, B. W.; Chen, F.; Mohideen, U. Precision measurement of the Casimir force using gold surfaces. Phys. Rev. A **2000**, 62, 052109.
- (45) Chen, Y.-J.; Tham, W. K.; Krause, D. E.; López, D.; Fischbach, E.; Decca, R. S. Stronger Limits on Hypothetical Yukawa Interactions in the 30–8000 nm Range. Phys. Rev. Lett. 2016, 116, 221102.
- (46) Casimir, H. B. G. On the Attraction Between Two Perfectly Conducting Plates. <u>Indag.</u> Math. **1948**, 10, 261–263.
- (47) Parsegian, V. A.; Weiss, G. H. Dielectric Anisotropy and the van der Waals Interaction between Bulk Media. The Journal of Adhesion 1972, 3, 259–267.
- (48) Wang, M.; Tang, L.; Ng, C. Y.; Messina, R.; Guizal, B.; Crosse, J. A.; Antezza, M.; Chan, C. T.; Chan, H. B. Strong geometry dependence of the Casimir force between interpenetrated rectangular gratings. Nature Communications **2021**, 12, 600.
- (49) Xu, Z.; Ju, P.; Gao, X.; Shen, K.; Jacob, Z.; Li, T. Observation and control of Casimir effects in a sphere-plate-sphere system. Nature Communications **2022**, 13, 6148.
- (50) Hopkins, J. C.; Podgornik, R.; Ching, W.-Y.; French, R. H.; Parsegian, V. A. Disentangling the Effects of Shape and Dielectric Response in van der Waals Interactions between Anisotropic Bodies. <u>The Journal of Physical Chemistry C</u> 2015, <u>119</u>, 19083–19094.
- (51) Hebestreit, E.; Frimmer, M.; Reimann, R.; Novotny, L. Sensing Static Forces with Free-Falling Nanoparticles. Phys. Rev. Lett. **2018**, 121, 063602.